

# Cosmic ray signatures of Dipole-Interacting Fermionic Dark Matter

Jae Ho Heo\* and C. S. Kim†

*Department of Physics and IPAP, Yonsei University, Seoul 120-479, Korea*

## Abstract

Cosmic ray signals from dipole-interacting dark matter annihilation are considered in the positron, antiproton and photon channels. The predicted signals in the positron channel could nicely account for the excess of positron fraction from Fermi LAT, PAMELA, HEAT and AMS-01 experiments for dark matter mass larger than 100 GeV with a boost (enhancement) factor of 30 – 80. No excess of antiproton over proton ratio at the experiments also gives a severe restriction for this scenario. The predicted signals as monoenergetic gamma-ray lines (monochromatic photons) for the region close to the Galactic center are investigated, and we show that they are in the current observational experimental constraint. To the end, the gamma-ray excess of recent tentative analyses based on Fermi LAT data and the potential probe of the monochromatic lines at a planned experiment, AMS-02, are also considered.

PACS numbers: 13.40.Em, 14.80.-j, 95.35.+d, 98.70.Sa

---

\*Electronic address: [jaeheo1@gmail.com](mailto:jaeheo1@gmail.com)

†Electronic address: [cskim@yonsei.ac.kr](mailto:cskim@yonsei.ac.kr)

## I. INTRODUCTION

The existence of the dark matter (DM), as the invisible matter interacting by the force of gravity, has been widely accepted by cosmological observations from the experiments: Cosmic Microwave Background (CMB) [1], Galactic Rotation Curves [2], Gravitational Lensing [3] and Massive Compact Halo Objects [4], and *etc.* About 83% of the matter (around 23% of the total energy density) in the universe is believed to be composed of the DM to account for the observations. However, the nature of DM is still completely unknown despite decades of detection efforts. Many possible explanations have been proposed. One of the alternative explanations from the point of view of particle physics is that the DM is composed of massive particles and its interaction with ordinary matter is very weak.

Recently several DM models<sup>1</sup> (inelastic DM [7, 8], asymmetric DM [9], form factor DM [10]) by magnetic dipole interaction have been considered. The DM in these models have a few states and have no direct interaction with the photon. The candidate particles could thus be stable and make up the invisible matter in our universe. On the other hand, the direct interaction with photon through magnetic dipole coupling has gotten some more attention [11–17] due to its plausibility. Most of works concentrated on direct detections of the DM. The main motivation of magnetic dipole interacting DM scenario is that the magnetic dipole coupling can be sizable compared to other electromagnetic couplings, because the magnetic dipole conserves the discrete symmetries like parity (P), time reversal (T), and charge conjugation (C) or its combinations.

In this work, we consider cosmic ray signatures (indirect detections) of the direct dipole-interacting DM with the shifted photon (hypercharge gauge boson  $B_\mu$ ). The cosmic ray signatures in the positron, anti-proton and photon channels are considered for the DM mass near the electroweak scale (10 – 1000 GeV), essentially around 100 GeV. The dimension-5 operator which induces the dipole interaction is  $\bar{\psi}\sigma_{\mu\nu}\psi B^{\mu\nu}$ , and it may be expressed about photon and  $Z$  boson in the standard model context since hypercharge gauge boson is a linear combination of photon and  $Z$  boson with Weinberg angle  $\theta_W$ . The relevant effective

---

<sup>1</sup> Actually these models have been built to explain the annual modulation signal from DAMA/NaI [5] and DAMA/LIBRA [6] experiments with null results from other experiments (there is no experimental evidence corroborating this signal yet). The scenario in Ref. [7] is especially interesting, because the signal appears electromagnetic energy deposit, not nuclear energy deposit, through the single photon emission by the decay of the excited state.

Lagrangian is given by

$$\mathcal{L}_{\text{eff}} = \frac{1}{2} \mu \bar{\psi} \sigma_{\mu\nu} \psi (F^{\mu\nu} - \tan \theta_W Z^{\mu\nu}), \quad (1)$$

where  $F^{\mu\nu}$  is the field strength for photon,  $Z^{\mu\nu}$  for  $Z$  boson and  $\mu$  is the magnetic dipole moment. The DM annihilations therefore proceed to the standard model particles via  $\gamma, Z$  exchanges. The annihilation processes were studied in Ref. [11] in detail, and here we take an advantage of the results (annihilation rates or branching ratios).

## II. COSMIC RAY SIGNATURES

The DM may annihilate at some point in Galaxy and produce the standard model particles. These produced particles then propagates in the interstellar medium. The anti-matters and photons have been considered to be the subject of indirect DM searches, because the anti-matters are rarely produced in astrophysical process and gamma rays can transport freely without energy loss or transmutation of the direction. They may thus provide important signatures of the DM in the Galaxy. Observations of such signals can reveal information on the microscopic nature of the DM.

The emissivity/energy (production rate or source for the signals)<sup>2</sup> at location  $\mathbf{x}$  from the Galactic center is obtained from the convolution over the various annihilation channels  $f$  of the annihilation rate  $\langle \sigma v \rangle_f$  with the differential yield (single particle spectra)<sup>3</sup>  $(dN^f/dT)_a$  for the final state particles  $a$ ,

$$Q_a(\mathbf{x}, T) = \frac{1}{4} B \langle \sigma v \rangle_f \left( \frac{dN^f}{dT} \right)_a \left( \frac{\rho(\mathbf{x})}{M} \right)^2, \quad (2)$$

where  $M$  is the DM mass,  $B$  is an overall boost (enhancement) factor and  $\rho(\mathbf{x})$  is the DM mass density at the location  $\mathbf{x}$ . The DM mass density about the location from Galactic center (DM halo profile) is not known, especially nearby center ( $\leq 100$  pc). The theoretically motivated ones are Navarro-Frenk White (NFW) [23], Moore [24], cored Isothermal [25],

---

<sup>2</sup> If the DM is produced with a primordial asymmetry like baryons, there would be almost no signals from DM-antiDM annihilations due to lack of anti-darkmatters (antiDMs). This source is for equal populations of the DM and antiDM, and hence our predicted signals will be upper limits of the predictions. Recently a mechanism of the DM-antiDM oscillations is suggested to re-equilibrate the populations at late times [18, 19].

<sup>3</sup> We use PYTHIA [20], as implemented in DarkSUSY [21] or MicrOMEGAs [22] program, to generate the differential yields (injected particle spectra).

and recently Einasto profiles [26, 27]. The kinetic energy is often approximated to the total energy  $E$ , in case that the particles are energetic. Notice that the factor  $\frac{1}{4}$  is different from the one of self annihilating DM.

The charged particles which are generated from the DM annihilation are predicted to come from the halo near the Sun, not too far from the Sun at least, because they may lose the energy while propagating through the Galactic halo. They are deflected by the Galactic magnetic field, and this property has been described by space diffusion [28]. The charged particles also suffer energy losses from synchrotron radiation and inverse Compton scattering. Solar modulation can induce a certain amount of energy losses. Their energy spectrum at the Earth, therefore, differs from the one produced at the source. The equation that describes the evolution of the energy distribution for the charged particles may be expressed as

$$\begin{aligned} \frac{\partial}{\partial t} \left( \frac{dn}{dT} \right)_a - \nabla \cdot \left( K(T) \nabla \left( \frac{dn}{dT} \right)_a \right) - \frac{\partial}{\partial T} \left( b(T) \left( \frac{dn}{dT} \right)_a \right) + \frac{\partial}{\partial z} \left( \text{sign}(z) V_C \left( \frac{dn}{dT} \right)_a \right) \\ = Q_a(\mathbf{x}, T) - 2h\Gamma_{ann}\delta(z) \left( \frac{dn}{dT} \right)_a, \end{aligned} \quad (3)$$

where  $dn/dT$  is the number density of particles per unit volume and energy. The second term accounts for the space diffusion with the energy dependent diffusion constant  $K(T)$ . The energy loss due to synchrotron radiation and inverse Compton scattering on CMB photons and on Galactic starlight is described in the third term with the rate of energy loss  $b(T)$ , and the fourth term deals convective wind. The last term accounts for the annihilation of the produced matters in the interstellar medium, H and He atoms, with annihilation rate  $\Gamma_{ann}$  in the disk of thickness  $2h \simeq 0.2$  kpc, and hence it is provided as a negative source term. The relevant coefficients were parameterized, and the established (transport) parameters have been estimated from the analysis of observed isotope ratios in cosmic rays, primarily the boron to carbon (B/C) ratio [29]. Three propagation models have been featured with the established parameters, and these propagation models correspond to minimal (MIN), medium (MED) and maximum (MAX) anti-proton fluxes [29, 30].

The number density  $dn/dT$  is obtained by solving Eq. (3) with the steady state condition  $\frac{\partial}{\partial t} \left( \frac{dn}{dT} \right)_a = 0$  and boundary conditions in a two-zone model [31], where the region of diffusion of cosmic rays is represented by a thick disk of thickness  $2L \simeq 5 - 20$  kpc and radius  $R \simeq 20$  kpc, and the thin Galactic disk lies in the middle and has a thickness  $2h$ , radius  $R$ . The boundary conditions are such that the number density vanishes at  $z = \pm L$  and at  $r = R$ .

## A. The Positron Channels

The propagation of positrons and electrons is dominated by space diffusion and energy losses,

$$-K(E)\nabla^2\left(\frac{dn}{dE}\right)_{e^+} - \frac{\partial}{\partial E}\left(b(E)\left(\frac{dn}{dE}\right)_{e^+}\right) = Q_{e^+}(\mathbf{x}, E). \quad (4)$$

This diffusion equation may be solved by the Green function formalism or the Bessel-transform method, and the solution results in the following form,

$$\left(\frac{dn}{dE}\right)_{e^+} = \frac{1}{b(E)} \int_E^M dE_S Q_{e^+}(\mathbf{x}_\odot, E_S) G_{e^+}(E, E_S), \quad (5)$$

where  $\mathbf{x}_\odot$  is the location of the Sun from the Galactic center. The function  $G_{e^+}(E, E_S)$  must fully encode the Galactic astrophysics from the input energy  $E_S$  to energy  $E(\leq E_S)$ , and the full expression of this function can be found in Ref. [30].

The positron flux is then given by

$$\phi_{e^+} = B \frac{v_{e^+}}{4\pi} \left(\frac{dn}{dE}\right)_{e^+} = B \frac{v_{e^+} \langle \sigma v \rangle_f}{16\pi b(E)} \left(\frac{\rho_\odot}{M}\right)^2 \int_E^M dE_S \left(\frac{dN^f}{dE}\right)_{e^+} G_{e^+}(E, E_S), \quad (6)$$

where  $\rho_\odot \simeq 0.4 \text{ GeV/cm}^3$  [32] is the DM density in the solar vicinity, and  $v_{e^+}$  is the velocity of the positron.

The enhancement may come from subhalo structure (dark clumps), and the non-perturbative Sommerfeld effect because one of force carriers is photon in this scenario. The enhancement by the Sommerfeld effect can be calculated from the original form in this case. We can split the dipole operator in energy and momentum dependent parts by the familiar Gordon decomposition,

$$\mu \bar{v}(p') \sigma^{\mu\nu} q_\nu u(p) = i\mu \bar{v}(p') (2M\gamma^\mu + (p' - p)^\mu) u(p). \quad (7)$$

In the energy dependent part, we have the same type of coupling with the DM mass dependence as electric charge. The original Sommerfeld enhancement factor is

$$S = \frac{\pi\alpha_\mu/v}{1 - e^{-\pi\alpha_\mu/v}} \underset{\alpha_\mu \gg v}{\sim} \frac{\pi\alpha_\mu}{v}, \quad (8)$$

where  $v$  is the DM velocity ( $\sim 10^{-3}$ ). In the original form,  $\alpha_\mu$  is the electric fine structure constant, but  $\alpha_\mu = 16\pi\mu^2 M^2$  in this case. We have the enhancement  $S \simeq 16$  for the DM mass of 100 GeV and magnetic dipole  $\mu \simeq 0.1 \text{ TeV}^{-1} (\sim 10^{-17} e\text{-cm})$ . The strength of magnetic dipole is, according to Ref. [11], almost constant for the DM mass larger than 100

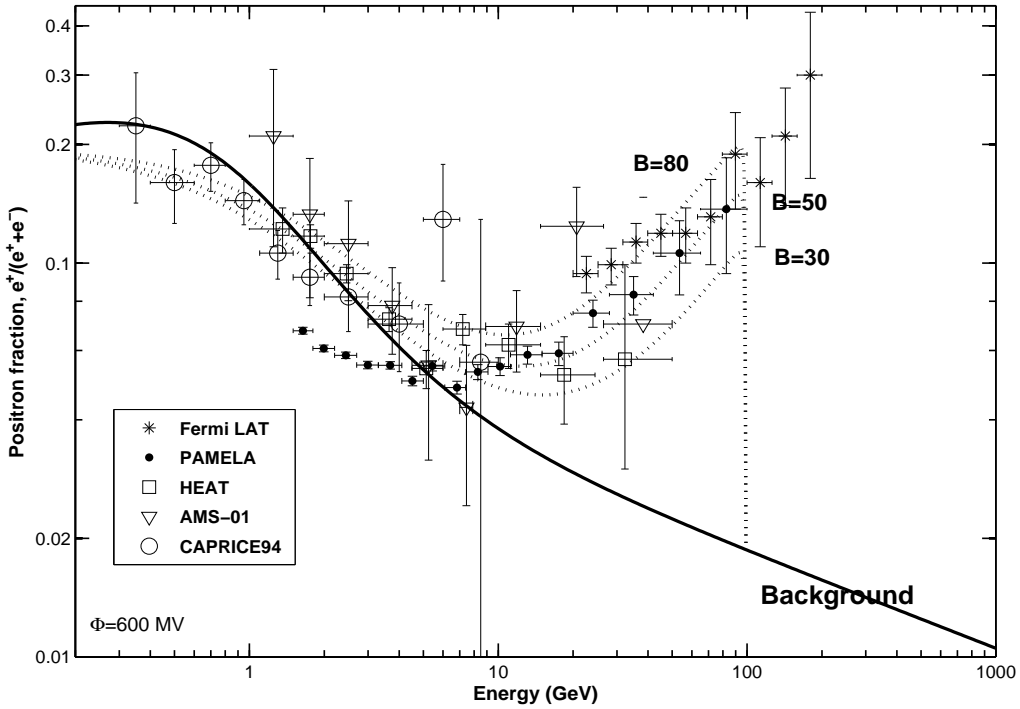


FIG. 1: Positron fraction from the annihilation of the fermionic dark matter particle. The boost factors have been chosen to provide qualitatively good fits to the data with dark matter mass 100 GeV. Shown are the background in solid-line and the experimental datasets of the PAMELA [35], HEAT [36], AMS-01 [37], Fermi LAT [38], and CAPRICES94 [39].

GeV, and thereby the enhancement increases in the square of the DM mass. Thanks to this reason, the fluxes, Eq.(6), must have the similar magnitude about the DM masses larger than 100 GeV because the fluxes are not scaled by the DM mass in our scenario. We notice that the fluxes are scaled by the DM mass in most of models, and large boost factors have been required for larger DM mass because the fluxes decrease in the square of the DM mass.

The positrons are affected by solar wind and lose energy while transporting in the solar system. This effect leads to a shift in the energy distribution between the interstellar spectrum (IS) and the spectrum at the top of the atmosphere (TOA). This modulation is considered for the predicted fluxes by the relation in force field approximation [33],

$$\phi_{e^+}^{\text{TOA}}(E) = \frac{E^2 - m_{e^+}^2}{(E + |Z|e\Phi)^2 - m_{e^+}^2} \phi_{e^+}^{\text{IS}}(E + |Z|e\Phi), \quad (9)$$

where  $|Z|$  is the magnitude of electric charge (1 in this case),  $e$  is the electric constant and  $\Phi$  is the Fisk potential, namely solar modulation parameter, which varies between 500 MeV and 1.2 GeV over the eleven-year solar cycle. Since experiments are usually undertaken near solar minimum activity, we choose  $\Phi = 600$  MeV (the Fisk potential for the PAMELA experiment) for our numerical analysis.

We show in Fig. 1 the predicted positron fractions for the boost factors,  $B = 30, 50, 80$ , with the computed background from Ref. [34] and several experimental data sets. The predicted fluxes have almost no difference in the halo profiles or the diffusion models. The predicted fractions exhibit a rather sharp distribution at  $E_{e^+} \simeq M$ , since our candidate can directly annihilate into electron and positron pair. The PAMELA [35] have shown a steep rise in the 10 – 100 GeV range in their measurements and confirmed the results of HEAT [36] and AMS-01 [37] experiments. Recently, the steep rise has been extended to 200 GeV with three more data points over 100 GeV at the Fermi LAT [38]. The predicted signals with the boost factor 30 – 80 nicely fit measurements of the PAMELA for the DM mass of around 100 GeV. An enhancement of about a factor of 16 comes from the Sommerfeld effect, and the rest, an enhancement factor of 2 – 5, is expected to come from subhalo structure (dark clumps). The typical subhalo boost factor has been predicted to be ten [40, 41] or twenty [42] at most. Our subhalo boost factors are in the reasonable range. We also have the difference between predictions and experimental measurements or background at low energies ( $\leq 10$  GeV). It has been noticed that solar modulation effect we consider has no charge-sign dependence and has to be modified. This must be a future study.

## B. The Anti-proton Channels

The propagation of anti-protons is dominated by diffusion and the effect of the Galactic wind. The energy spectrum of anti-protons is obtained by solving the following diffusion equation,

$$\frac{\partial}{\partial z} \left( \text{sign}(z) V_C \left( \frac{dn}{dT} \right)_{\bar{p}} \right) - \nabla \cdot \left( K(T) \nabla \left( \frac{dn}{dT} \right)_{\bar{p}} \right) = Q_a(\mathbf{x}, T) - 2h\Gamma_{ann}\delta(z) \left( \frac{dn}{dT} \right)_{\bar{p}}. \quad (10)$$

An important difference with the positron case is that energy loss of anti-protons is negligible, because anti-protons are more massive and hence it is absent in the diffusion equation (10).

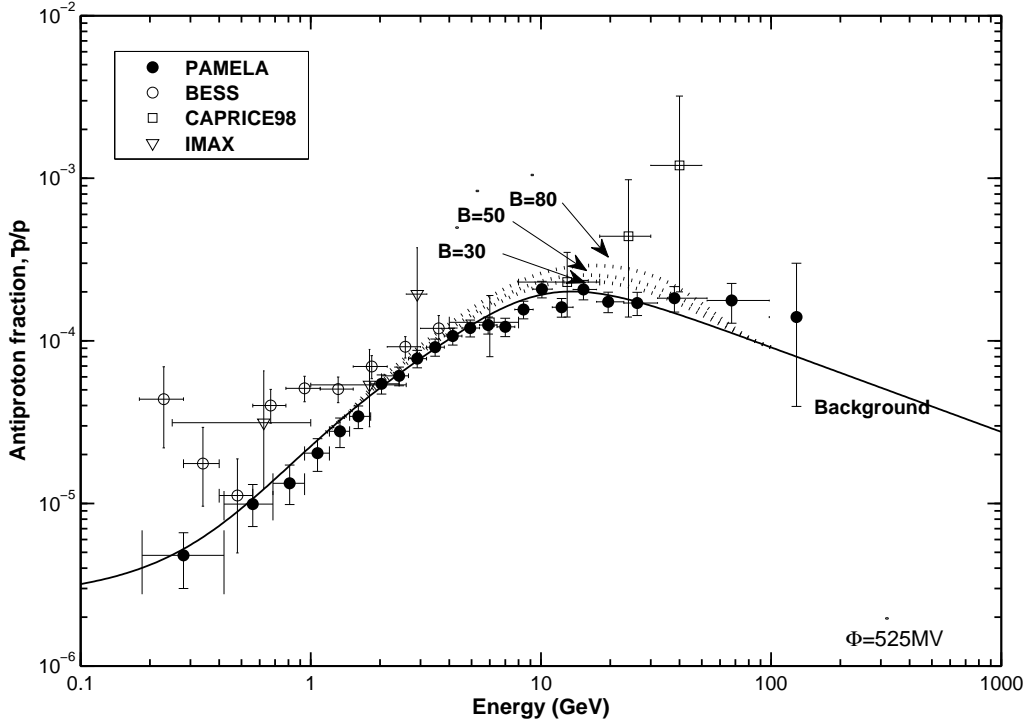


FIG. 2: Antiproton over proton ratio as a function of kinetic energy. Shown are the background in solid-line and the experimental data sets of the PAMELA [46], BESS [47], CAPRICE98 [48] and IMAX [49].

The anti-proton flux is then given by

$$\phi_{\bar{p}} = B \frac{v_{\bar{p}}}{4\pi} \left( \frac{dn}{dT} \right)_{\bar{p}} = B \frac{v_{\bar{p}} \langle \sigma v \rangle_f}{16\pi} \left( \frac{dN^f}{dT} \right)_{\bar{p}} \left( \frac{\rho_{\odot}}{M} \right)^2 G_{\bar{p}}(T), \quad (11)$$

where the function  $G_{\bar{p}}(T)$  encodes all the astrophysics, and the full expression can be found in Refs. [43, 44].

Fig. 2 shows the predicted ratios of anti-proton over proton with the computed background [45] and several experimental measurements. As in the case of the positrons, the predictions have almost no difference in the halo profiles, but it is sensitive to the propagation models. The predictions in the MIN propagation model are selected, and they are within the unobservational range. However, this scenario is most likely ruled out for other propagation models<sup>4</sup>, MED and MAX, because the predicted fluxes in MED or MAX

<sup>4</sup> To be strict, the MED propagation model can also be viable because of the uncertainty of the transport

propagation models are about ten or one hundred times larger than the ones in the MIN propagation models.

### C. The Gamma Ray Channels

The production of gamma-rays has been considered to be a very important channel to search for the DM signals, since they travel in straight lines and can travel greater distances without energy loss. For these reasons, they contain spectral and directional information that can be well measured. The gamma-ray flux from the DM annihilations at a given photon energy from a direction that forms an angle  $\psi$  between the direction of the Galactic center and that of observation is accounted for by the line-of-sight (los) integration method,

$$\phi_\gamma = B \frac{\langle\sigma v\rangle_f}{16\pi M^2} \left(\frac{dN^f}{dE}\right)_\gamma \int_{\text{los}} \rho^2(r(s, \psi)) ds, \quad (12)$$

where  $r = \sqrt{r_\odot^2 + s^2 - 2r_\odot s \cos\psi}$  is the Galactocentric distance. In terms of the galactic latitude  $b$  and longitude  $l$ , one has  $\cos\psi = \cos b \cos l$ . The coordinate  $s$  parameterizes the distance from the Sun along the line-of-sight.

This form can be reduced to

$$\phi_\gamma \simeq 8.31 \times 10^{-11} \text{ (cm}^2 \cdot \text{sr} \cdot \text{s)}^{-1} \cdot \frac{B \langle\sigma v\rangle_f}{10^{-26} \text{ cm}^3 \text{s}^{-1}} \left(\frac{100 \text{ GeV}}{M}\right)^2 \left(\frac{dN^f}{dE}\right)_\gamma \cdot \bar{J}_{\Delta\Omega}, \quad (13)$$

where  $\bar{J}_{\Delta\Omega}$  is a dimensionless line-of-sight integral averaged over the solid angle  $\Delta\Omega$  and is defined by

$$\bar{J}_{\Delta\Omega} = \frac{1}{\Delta\Omega} \int J(\psi) d\Omega, \quad (14)$$

with

$$J(\psi) = \int \frac{\rho^2(r) ds}{\rho_\odot^2 r_\odot}. \quad (15)$$

In addition to the continuum emission, the direct DM annihilations produces  $\gamma\gamma$  and  $\gamma Z$  final states<sup>5</sup> in this scenario, in which Feynman diagrams are shown in Fig. 3. Such processes would yield the very distinctive feature of monoenergetic gamma-ray lines (monochromatic

---

parameters. The parameters are assigned to the best fit of cosmic ray B/C data [29]. However, the assigned values of transport parameters may differ by one order of magnitude.

<sup>5</sup> The production of the single  $\gamma$  or  $Z$  final state is prohibited, because this process is impossible to conserve energy and momentum together.

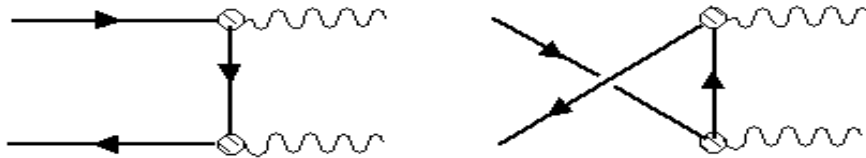


FIG. 3: Feynman diagrams for annihilation of dark matter to one-photon or two-photons. The hatched circles indicate the dipole couplings.

photons) with an energy  $E_\gamma = M$  or  $M(1 - m_Z^2/(2M)^2)$ . The full annihilation rates for the production of  $\gamma\gamma$  are  $\langle\sigma v\rangle_{\gamma\gamma} = \mu^4 M^2/2\pi$  and  $\langle\sigma v\rangle_{\gamma Z} = \mu^4 M^2 \beta_Z^2 \tan^2 \theta_W/4\pi$  for  $\gamma Z$ . The contributions for  $\gamma\gamma$  and  $\gamma Z$  final states are suppressed by the magnetic dipole  $\mu^4$ , and the  $\gamma Z$  final state has an additional suppression with Weinberg angle  $\tan^2 \theta_W$ .

We restrict our analysis to the possible signals from the Galactic halo as in the case of the positrons for a complementarity, and hence the same boost factors<sup>6</sup>  $B = 30, 50, 80$  are selected. We compare our predictions to experimental observations in two stringent cases. One is a process that may contribute to the extragalactic gamma-ray background (EGB). The other is a process to satisfy the experimental exclusion limit of the Fermi LAT [50], in the case that astrophysical sources account for the EGB in entire energy range.

Fig. 4 shows the predicted gamma-ray spectra as a function of photon energy in the region  $0^\circ \leq \ell \leq 360^\circ$ ,  $|b| \geq 10^\circ$ . The spectra are superimposes of the continuum and monoenergetic gamma-rays at the DM mass of 100 GeV. The spectra have almost no difference in the halo profiles. The EGB from the Fermi LAT [50] is given by

$$E_\gamma^2 \phi_\gamma \simeq 5.5 \times 10^{-7} \left( \frac{E}{1\text{GeV}} \right)^{-0.41} (\text{cm}^2 \cdot \text{sr} \cdot \text{s})^{-1} \text{GeV}. \quad (16)$$

The same type of background from the analysis of the EGRET measurements is also described [51] with the one from the first analysis [52]. The predicted spectra are within the EGB, and we might have a signature if it can be disentangled from astrophysical ones. In addition, we check if our prediction can account for the EGRET anomaly which is not con-

<sup>6</sup> The enhancements can be different in each channel on the subhalo structure. Here we select the same boost factors in the assumption that the enhancements by the subhalo structure are not too different in each channel.

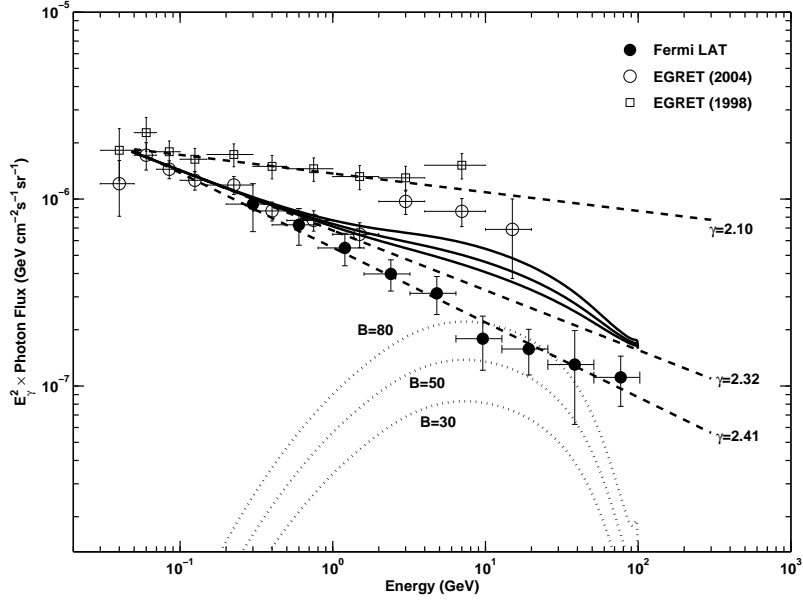


FIG. 4: The gamma-ray spectrum from Galactic halo for dark matter mass of 100 GeV and the region,  $0^\circ \leq \ell \leq 360^\circ, |b| \geq 10^\circ$ . Shown are the experimental data sets from the Fermi LAT and EGRET with their fitted spectral indices.

firmed at the Fermi LAT. Our predictions are softer to explain the observation of the EGB, and the more enhancement would be needed.

The predicted fluxes have to be within the uncertainty of Fermi LAT data, in the case that the EGB is accounted for by astrophysical sources in entire energy range. Fig. 5 shows the predicted fluxes with 90%, 95% and 99% experimental exclusion limits of the Fermi LAT, which are estimated from the data table in Ref. [50]. The predictions are under exclusion limits and are satisfied with the current unobservable experimental constraint.

The Galactic center or the region close to that must be the most complex regions in the Galaxy due to many possible sources and the difficulty to model the diffuse emission. Hence, it may be very difficult to disentangle possible DM annihilation signals from the background fluxes. The monochromatic gamma-ray lines appeared from DM annihilations could provide smoking-gun signatures for these regions, because the line signals cannot be mistaken for astrophysical source.

Fig. 6 shows the predicted annihilation rate for  $\gamma\gamma$  and  $\gamma Z$  final states as a function of the

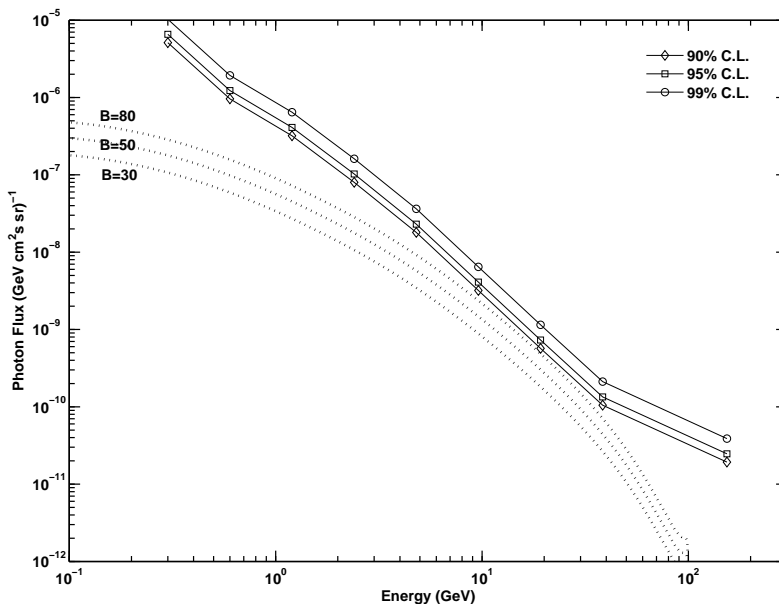


FIG. 5: The gamma-ray flux from Galactic halo for dark matter mass of 100 GeV and the target region  $0^\circ \leq \ell \leq 360^\circ, |b| \geq 10^\circ$  with 90%, 95% and 99% experimental exclusion limits of the Fermi LAT.

DM mass. The Sommerfeld effect is included, but not the subhalo structure. The strength of DM magnetic dipole is chosen to satisfy the relic density from Ref. [11]. The curves given for the NFW, Einasto, and isothermal DM distributions are 95% C.L. upper limits of Fermi LAT [53] for the region  $|b| \geq 10^\circ$  plus a  $20^\circ \times 20^\circ$  centered at the Galactic center. The predicted annihilation rates are approximately  $4.0 \times 10^{-29} \text{ cm}^3/\text{s}$  at  $E_\gamma \simeq 100 \text{ GeV}$  for the  $\gamma\gamma$  final state and  $4.0 \times 10^{-30} \text{ cm}^3/\text{s}$  for the  $\gamma Z$  final state at  $E_\gamma \simeq 80 \text{ GeV}$ . Otherwise, the estimated upper limits at the Fermi LAT are  $10^{-27} - 10^{-26} \text{ cm}^3/\text{s}$  for both final states, depending on the DM mass and the halo profiles. The predictions are two or three orders smaller than the experimental upper limits. However, our predictions can be enhanced if dense DM clumps are considered in regions close to the Galactic center. Recently, the authors in Refs. [54, 55] pointed out the gamma-ray excess,  $1 - 3 \times 10^{-27} \text{ cm}^3/\text{s}$ , around 130 GeV in the spectrum based on these measurements with 4.5 or  $6\sigma$  statistical significance. Our predictions with the subhalo boost factor of about 100 can account for the gamma-ray excess.

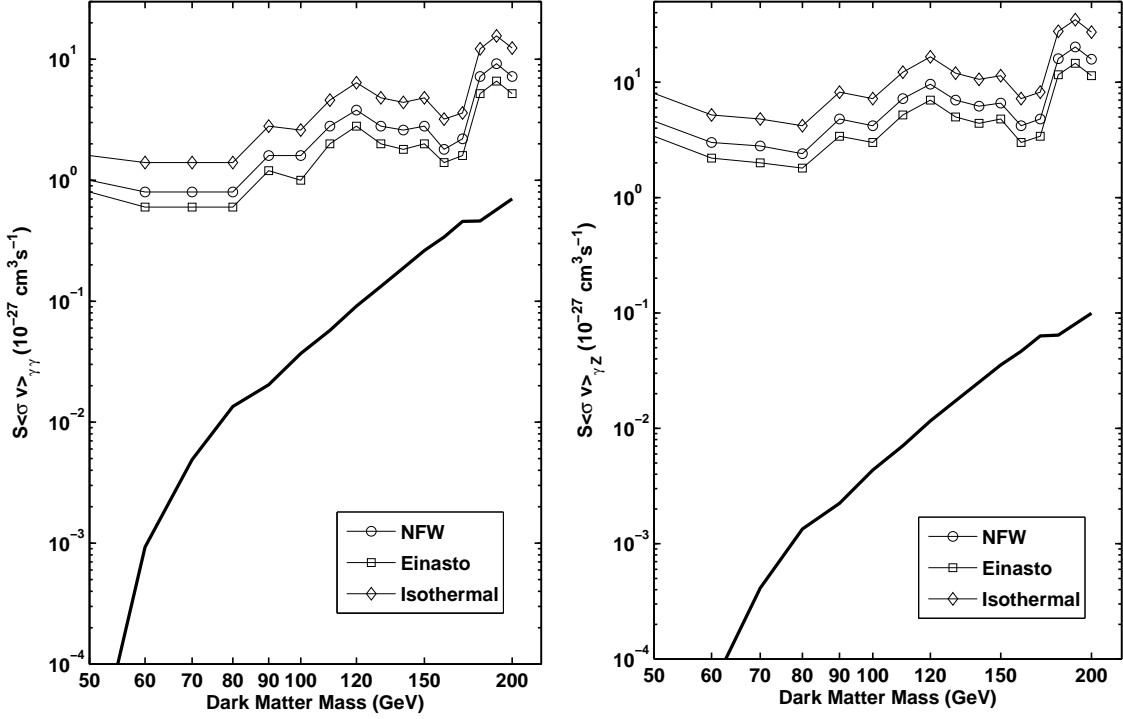


FIG. 6: Annihilation rates with Sommerfeld enhancement factor  $S$  for dark matter annihilation to  $\gamma\gamma$  or  $\gamma Z$ . Shown are the 95% C.L. upper limits of the Fermi LAT for the region  $|b| \geq 10^\circ$  plus a  $20^\circ \times 20^\circ$  centered at the Galactic center.

One of the reasons we mostly get the low predictions for sharp peaks is due to the relatively poor energy resolution. The current energy resolution of the Fermi LAT is 11 – 13% [53] for the full width at half maximum. The energy resolution could be as better as 1.5 – 2% for a planned experiment, AMS-02 [56], in which the upper limits of annihilation rate will be  $10^{-30} - 10^{-29} \text{ cm}^3/\text{s}$ . Our predicted signals are in the potential probe at the AMS-02.

### III. CONCLUSION

We considered cosmic ray signals in the positron, anti-proton and photon channels of dipole-interacting DM annihilation. The predicted signals in the positron channel could nicely account for the excess of positron fraction from Fermi LAT, PAMELA, HEAT and AMS-01 experiments for the DM mass larger than 100 GeV with a boost factor of 30 – 80.

We estimated that an enhancement of about a factor of 16 would come from the Sommerfeld non-perturbative effect and the rest, an enhancement factor of  $2 - 5$ , from subhalo structure (dark clumps). The predicted signals have almost no dependence on the DM mass because of the Sommerfeld effect. No excess of anti-proton over proton ratio at the experiments also gives a severe restriction for our scenario. This scenario must be viable for MIN Galactic propagation model, but likely ruled out for other propagation models, MED and MAX. The predicted signals from the Galactic halo in the region  $0^\circ \leq \ell \leq 360^\circ, |b| \geq 10^\circ$ , and signals as the monoenergetic gamma-ray lines (monochromatic photons) for the region ( $|b| \geq 10^\circ$  plus a  $20^\circ \times 20^\circ$  centered at the Galactic center) close to Galactic center were also considered. The predicted signals from the Galactic halo must be in the current unobservable experimental constraint, and the signals for the region near Galactic center as monoenergetic lines are under experimental exclusion limits of the Fermi LAT. The gamma-ray excess  $1 - 3 \times 10^{-27} \text{cm}^3/\text{s}$  around 130 GeV, which authors in Refs. [54, 55] pointed out, could be accounted for in this scenario with the subhalo boost factor of about 100. Our predicted signals as monoenergetic lines for the region near Galactic center are also in the potential probe at a planned experiment, AMS-02, with the better experimental method.

### Acknowledgments

The work was supported by the National Research Foundation of Korea (NRF) grant funded by Korea government of the Ministry of Education, Science and Technology (MEST) (No. 2011-0027275), (No. 2012-0005690) and (No. 2011-0020333).

- 
- [1] E. Komatsu *et al.* [WMAP Collaboration], *Astrophys. J. Suppl.* **192**, 18 (2011), [astro-ph/1001.4538](#).
  - [2] A. Borriello, P. Salucci, *Mon. Not. R. Astro. Soc.* **323**, 285 (2001).
  - [3] H. Hoekstra, H. Yee, M. Gladders, *New Astron. Rev.* **46**, 767 (2002).
  - [4] C. Alcock *et al.* [MACHO Collaboration], *Astrophys. J.* **542**, 281 (2000), [astro-ph/0001272](#).
  - [5] R. Bernabei *et al.* [DAMA Collaboration], *La Rivista del Nuovo Cimento* 26 n.1, 1 (2003); *Int. J. Mod. Phys. D* **13**, 2127 (2004), [astro-ph/0501412](#).
  - [6] R. Bernabei *et al.* [DAMA Collaboration], *Eur. Phys. J. C* **56**, 333 (2008), [astro-ph/0804.2741](#).

- [7] B. Feldstein, P. W. Graham, S. Rajendran, Phys. Rev. D **82**, 075019 (2010), hep-ph/1008.1988.
- [8] T. Lin, D. P. Finkbeiner Phys. Rev. D **83**, 083510 (2011), astro-ph/1011.3052; S. Chang, N. Weiner, I. Yavin, Phys. Rev. D **82**, 125011 (2010), hep-ph/1007.4200; J. Shu, P. Yin, S. Zhu, Phys. Rev. D **81**, 123519 (2010), hep-ph/1001.1076; S. Chang, G.D. Kribs, D. Tucker-Smith, N Weiner, Phys. Rev. D **79**, 043513 (2009), hep-ph/0807.2250.
- [9] H. An, S. Chen, R.M. Mohapatra, S. Nussinov, Y Zhang, Phys. Rev. D **82**, 023533 (2010), hep-ph/1004.3296 ; M. Pospelov, A. Ritz, Phys. Lett. B **671**, 391 (2009), hep-ph/0810.1502 .
- [10] B. Feldstein, A.L. Fitzpatrick, E. Katz *et al.*, J. Cosmol. Astropart. Phys. **03**, 029 (2010); S. Chang, A. Pierce, N. Weiner, J. Cosmol. Astropart. Phys. **01**, 006 (2010).
- [11] Jae Ho Heo, Phys. Lett. B **693**, 255 (2010), hep-ph/0901.3815 ; Phys. Lett. B **702**, 205 (2011), hep-ph/0902.2643.
- [12] M. Pospelov, T. Veldhuis, Phys. Lett. B **480**, 181 (2000), hep-ph/0003010.
- [13] K. Sigurdson, M. Doran, A. Kurylov, R.R. Caldwell, M. Kamionkowski, Phys. Rev. D **70**, 083501 (2004) [Erratum-ibid. D 73, 089903 (2006)], hep-ph/0406355.
- [14] V. Barger, W. -Y. Keung, D. Marfatia, Phys. Lett. B **696**, 74 (2011), hep-ph/1007.4345.
- [15] W.S. Cho, J.-H. Huh, I.-W. Kim, J.E. Kim, B. Kyae, Phys. Lett. B **687**, 6 (2010) [Erratum-ibid. B **694**, 496 (2011)], hep-ph/1001.0579.
- [16] T. Banks, J.-F. Fortin, S. Thomas, hep-ph/1007.5515.
- [17] E.D. Nobile, C. Kouvaris, P. Panci, F. Sannino, J. Virkajarvi, hep-ph/1203.6652.
- [18] S. Tulin, H.-B. Yu, K.M. Zurek, hep-ph/1202.0283.
- [19] M. Cirelli, P. Panci, G. Servant, G. Zaharijas, J. Cosmol. Astrophys. **1203**, 015 (2012), hep-ph/1110.3809.
- [20] T. Sjostrand, S. Mrenna, P. Skands, Comput. Phys. Commun. 178, 852 (2008), hep-ph/0710.3820.
- [21] P. Gondolo, J. Edsjo, P. Ullio, L. Bergstrom, M. Schelke, E.A. Baltz, J. Cosmol. Phys. **0407**, 008 (2004), astro-ph/0406204.
- [22] G. Belanger, F. Boudjema, P. Brun, A. Pukhov, S. Rosier-Lees, P. Salati, A. Semenov, Comput. Phys. Commun. **182**, 842 (2011), hep-ph/1004.1092.
- [23] J.F. Navarro, C.S. Frenk, S.D.M. White, Astrophys. J. **490**, 493 (1997), astro-ph/9611107.
- [24] B. Moore, F. Governato, T. Quinn, J. Stadel, G. Lake, Astrophys. J. **499**, L5 (1998); J. Diemand, B. Moore, J. Stadel, Mon. Not. R. Astron. Soc. **353**, 624 (2004), astro-ph/0402267.

- [25] J.N. Bahcall, R.M. Soneira, *Astrophys. J. Suppl.* **44**, 73 (1980).
- [26] J. Einasto, *Trudy Inst. Astroz. Alma-Ata* **51**, 87 (1965).
- [27] J.F. Navarro *et al.*, astro-ph/0810.1522.
- [28] F. Casse, M. Lemoine, G. Pelletier, *Phys. Rev. D* **65**, 023002 (2002), astro-ph/0109223.
- [29] F. Donato, N. Fornengo, D. Maurin, P. Salati, R. Taillet, *Phys. Rev. D* **69**, 063501 (2004), astro-ph/0306207; D. Maurin, F. Donato, R. Taillet, P. Salaati, *Astrophys. J.* **555**, 585 (2001), astro-ph/0101231.
- [30] T. Deliahaye, R. Lineros, F. Donato, N. Fornengo, P. Salati, *Phys. Rev. D* **77**, 063527 (2008), astro-ph/0712.2312.
- [31] F. Donato, D. Maurin, P. Salati, A. Barrau, G. Boudoul, R. Taillet, *Astrophys. J.* **563**, 172 (2001), astro-ph/0103150.
- [32] R. Catena, P. Ullio, *J. Cosmol. Astropart. Phys.* **08**, 004 (2010), astro-ph/0907.0018.
- [33] L.J. Gleeson, W.I. Axford, *Astropart. Phys.* **154**, 1011 (1968) ; **149**, L115 (1967).
- [34] I.V. Moskalenko, A.W. Strong, *Astrophys. J.* **149**, L115 (1998).
- [35] O. Adriani *et al.* [PAMELA Collaboration], *Nature* **458**, 607 (2009) ; *Astropart. Phys.* **34**, 1 (2010), astro-ph/1001.3522.
- [36] S.W. Barwick *et al.* [HEAT Collaboration], *Astrophys. J.* **482**, L191 (1997), astro-ph/9703192.
- [37] M. Aguilar *et al.* [AMS-01 Collaboration], *Phys. Lett. B* **646**, 145 (2007).
- [38] M. Ackermann *et al.* [Fermi LAT Collaboration], *Phys. Rev. Lett.* **108**, 011103 (2012), astro-ph/1109.3521.
- [39] M. Boezio *et al.* [WIZARD Collaboration], *Astrophys. J.* **532**, 653 (2000).
- [40] J. Diemand *et al.*, *Nature* **454**, 735 (2008), astro-ph/0805.1244; J. Diemand, M. Kuhlen, P. Madau, *Astrophys. J.* **657**, 262 (2007), astro-ph/0611370.
- [41] M. Cirelli, R. Franceschimi, A. Strumia, *Nucl. Phys. B* **800**, 204 (2008), astro-ph/0802.3378.
- [42] K. Kadota, K. Freese, P. Gondolo, *Phys. Rev. D* **81**, 115006 (2010), hep-ph/1003.4442.
- [43] P. Chardonnet, G. Mignola, P. Salati, R. Taillet, *Phys. Lett. B* **384**, 161 (1996), astro-ph/9606174.
- [44] L. Bergstrom, J. Edsjo, P. Ullio, *Astrophys. J.* **526**, 215 (1999), astro-ph/9902012.
- [45] A.M. Lionetto, A. Morselli, V. Zdravkovic, *J. Cosmol. Astropart. Phys.* **09**, 010 (2005), astro-ph/0502406 ; T. Bringmann, P. Salati, *Phys. Rev. D* **75**, 083006 (2007), astro-ph/0612514.

- [46] O. Adriani *et al.* [PAMELA Collaboration], Phys. Rev. Lett. **105** (12), 121101 (2010), astro-ph/1007.0821.
- [47] Y. Asaoka *et al.*, Phys. Rev. Lett. **88**, 051101 (2002), astro-ph/0109007.
- [48] M. Boezio *et al.* [WIZARD/CAPRICE Collaboration], Astrophys. J. **561**, 787 (2001), astro-ph/0103513
- [49] J.W. Mitchell *et al.*, Phys. Rev. Lett. **76**, 3057 (1996).
- [50] A.A. Abdo *et al.* [Fermi LAT Collaboration], Phys. Rev. Lett. **104**, 101101 (2010), astro-ph/1002.3603.
- [51] A.W. Strong, I. V. Moskalenko, O. Reimet, Astrophys. J. **613**, 956 (2004), astro-ph/0405441; Astrophys. J. **613**, 962 (2004), astro-ph/0406254.
- [52] P. Sreekumar *et al.* [EGRET Collaboration], Astrophys. J. **494**, 523 (1998), astro-ph/9709257.
- [53] M. Ackermann *et al.* [Fermi LAT Collaboration], astro-ph/1205.2739; A.A. Abdo *et al.* [Fermi LAT Collaboration], Phys. Rev. Lett. **104**, 091302 (2010), astro-ph/1001.4836.
- [54] C. Weniger, hep-ph/1204.2797.
- [55] E. Tempel, A. Hektor, M. Raidal, hep-ph/1205.1045.
- [56] A. Kounine, astro-ph/1009.5349; <http://ams.cern.ch>.